HETEAC-Flex Model: Comparative Evaluation of 6 Forward model configurations for Dust Cases using Ground-based Lidar Observations in Limassol

Athina Savva [*a,b], Argyro Nisantzi [a,b], Maria Poutli[a,b], Albert Ansmann[3], Diofantos G. Hadjimitsis [a,b], Rodanthi E. Mamouri [a,b]

[a] Eratosthenes Centre of Excellence, 3012 Limassol, Cyprus; [b] Department of Civil Engineering & Geomatics, Cyprus University of Technology, 3036 Limassol, Cyprus; [c] Leipniz Institute for Tropospheric Research, 04318 Leipzig, Germany

*athina.savva@eratosthenes.org.cy; phone +357 993959315; eratosthenes.org.cy

ABSTRACT

The Cyprus Atmospheric Remote Sensing Observatory National Facility (CARO NF) of Eratosthenes Centre of Excellence plays a key role in atmospheric research and the characterization of atmospheric conditions in the Eastern Mediterranean. Equipped with cutting-edge remote sensing instruments including a Polly^{XT} Polarization Raman Lidar, a Cloud Radar and a Solar Infrastructure, CARO provides critical observations for studying aerosol properties, cloud dynamics, and radiative processes. Its advanced capabilities make it an essential ground-based station for satellite validation studies, particularly in the context of the EarthCARE mission (ESA/JAXA). To ensure compatibility between ground-based observations and satellite measurements, the HETEAC-Flex model, introduced by A. A. Floutsi et al., 2024 [1] have been applied for the aerosol layer classification. This model was created to validate the aerosol classification of ATLID (ATmospheric LIDar) measurements, onboard EarthCARE, by providing a robust comparison framework. Based on an Optimal Estimation Method (OEM) HETEAC-Flex provides six forward retrieval modes, each incorporating different sets of optical properties including Particle linear depolarization ratio at 355, 532 nm, Lidar ratio at 355, 532 nm, Extinction-related Ångström exponent at 355/532 nm and the Backscatter-related color ratio for 532/1064 nm. The typing scheme enables the identification of four aerosol components of aerosol mixtures, absorbing and less-absorbing fine-mode particles and spherical and non-spherical coarse-mode particles (FSA, FSNA CS, CNS, respectively).
CARO's Polly^{XT} lidar in Limassol can retrieve all the optical properties needed for the utilization of all the six retrieval modes. In this study, we apply the HETEAC-Flex model to several dust cases recorded in Limassol between the period 2021-2024, aiming to determine which retrieval mode is the optimal for the characterizing dust aerosol layers.

Keywords: HETEAC-Flex, Dust Cases, Aerosol Characterization, Lidar, Limassol

1. INTRODUCTION

1.1 Study Area

Cyprus, an island located in the Eastern Mediterranean, is influenced by both fine and coarse-mode atmospheric aerosols originating from nearby and distance natural and anthropogenic sources. The Middle East and North Africa (MENA) region are positioned in the global dust belt (West Africa to Arabian Peninsula), significantly contributes to short and long-term transport of desert dust, affecting regularly Cyprus and neighbouring Mediterranean areas [2]. Desert dust storms (DDS) mostly occur at the end of winter and during spring (February-May) [3]. A key area of research is the vertically resolved characterization of aerosols in the heavily polluted eastern Mediterranean region focused on the vertical distribution of aerosols and their interplay with atmospheric dynamics, clouds and precipitation [4]. This area frequently experiences complex aerosol mixtures, regular occurrences of anthropogenic haze, desert, biogenic matter and agricultural particles [4, 5, 6, 7, 8, 9].

Eleventh International Conference on Remote Sensing and Geoinformation of the Environment (RSCy2025), edited by Andreas Christofi, et al., Proc. of SPIE Vol. 13816 · © The Authors. Published under a Creative Commons Attribution CC-BY 4.0 License · doi: 10.1117/12.3073308

1.2 HETEAC-Flex model

A Hybrid End-to-End Aerosol Classification (HETEAC) model was developed to facilitate a common aerosol characterization from the EarthCARE aerosol products throughout of the processing chain [10]. The model is a combination of a hybrid experimental and theoretical approach and simulates aerosol optical, microphysical and radiative parameters end to end of the predefined particles [11]. To ensure compatibility between ground-based observations and satellite measurements, the HETEAC-Flex model, introduced by A. A. Floutsi et al., 2024 [1] have been applied for the aerosol layer classification and it is based on HETEAC model. One of the objectives of the creation of this model is to validate the aerosol classification of ATLID measurements, onboard EarthCARE, by providing a robust comparison framework [1].

The HETEAC-flex model is a versatile aerosol classification algorithm due to its applicability to both ground-based and spaceborne lidars' derived intensive aerosol properties retrievals.
Optimal estimation method (OEM) is the framework that the model employs to retrieve aerosol mixtures from lidars [12]. This method provides adaptability also to different lidar system configurations and wavelengths. The general concept of the optimal estimation method is presented in Figure 1.

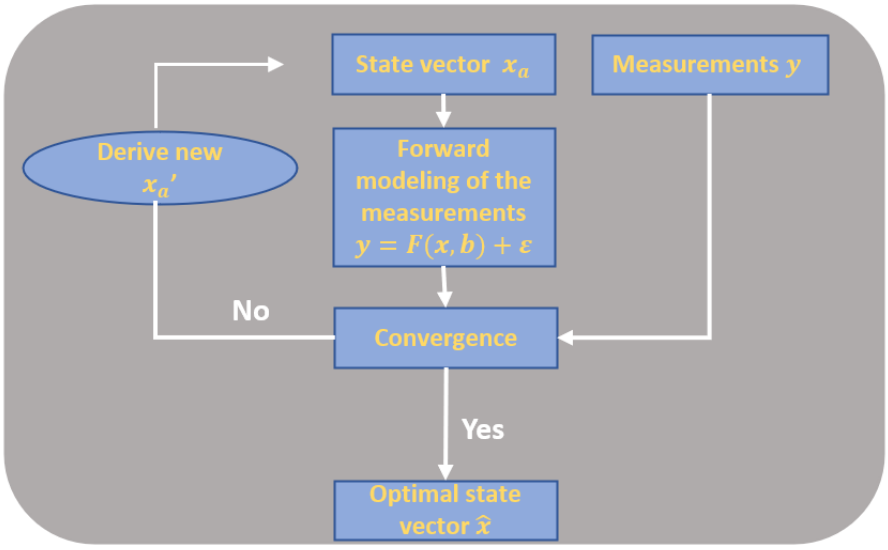

Figure 1. Optimal estimation method general concept. Where, x_a: a priori state vector (initial guess); y: measurement vector (observed data); F(x, b): forward model simulating measurements as a function of state vector x and model parameters b; ε: measurements corresponding error; $\hat{x}$: optimal (retrieved) state vector after convergence.

HETEAC-Flex model provides six forward model configurations, each incorporating different sets of optical properties making this feature critically significant for the utilization of different types of lidars. Each retrieval mode uses a combination of the following parameters including Particle linear depolarization ratio at 355, 532 nm, Lidar ratio at 355, 532 nm, Extinction-related Ångström exponent at 355/532 nm and the Backscatter-related color ratio for 532/1064 nm with their standard deviations [1]. In Table 1, the forward model configurations or else retrieval modes with input parameters are presented.
Four fundamental aerosol components enable the identification of aerosol mixtures forming the classification in absorbing and less-absorbing fine-mode particles (FSA, FSNA) and spherical and non-spherical coarse-mode particles (CS, CNS) respectively [1]. The algorithm can retrieve the relative volume contributions, the volume size distribution and the refractive index of the four aerosol components, which are important for characterizing the atmospheric conditions of the region and assessing the Earth's radiation balance [13].

Table 1. Forward model configurations with input parameters. Where, δ_{355}, δ_{532}: Particle linear depolarization ratio at 355 nm and 532 nm, respectively; S_{355}, S_{532}: Lidar ratio at 355 nm and 532 nm; $Å_{355/532}$: Ångström exponent between 355 nm and 532 nm; $C_{\beta 532/1064}$: Color ratio of backscatter coefficients at 532 nm and 1064 nm.

Retrieval modes	Parameters

1	δ_{355}, S_{355}
2	δ_{532}, S_{532}
3	δ_{355}, S_{355}, $A_{355/532}$
4	δ_{532}, S_{532}, $C_{\beta 532/1064}$
5	δ_{355}, S_{355}, δ_{532}, S_{532}
6	δ_{355}, S_{355}, $A_{355/532}$ δ_{532}, S_{532}, $C_{\beta 532/1064}$

In previous studies HETEAC-Flex model has been used in cases utilizing Ground-based lidars. A desert dust case from A-LIFE (Absorbing aerosol layers in a changing climate: ag-ing, LIFEtime and dynamics) campaign in Limassol, Cyprus was analysed by the model for the six retrieval configuration modes. Also, a case with two different aerosol layers from SAMUM-2 campaign in Cavo Verde which also compared with POLIPHON (polarization- lidar photometer networking) method [14, 15] which ensured the consistency of the model [1]. A seasonal distribution of the aerosol components from a two-year time series of Polly^{XT} lidar Raman nighttime observations in Haifa, Israel has been analysed utilizing HETEAC-flex model [16]. For this study, 1–2-hour averaged data analysed based on the availability at least one wavelength either 355 nm, 532 nm, or both, of the particle linear depolarization ratio and the lidar ratio. The findings of the study for the Haifa site indicate that coarse-mode spherical particles (e.g., sea salt) prevailing in summer, autumn and winter, fine-mode aerosols (e.g., industrial - pollution) contributed year-round and coarse non-spherical (e.g., desert dust) are dominant aerosols during spring period [16].

2. INSTRUMENTATION & METHODOLOGY

2.1. Data Selection and Preprocessing

The analysis is based on optical property data obtained from the multiwavelength Polly^{XT} (POrtabLe Lidar sYstem) Raman Polarization Lidar [17] system located in Limassol, Cyprus Limassol (34.677° N, 33.0375° E, 2.8 m above sea level, a.s.l.). The Lidar is part of the Cyprus Atmospheric Remote Sensing Observatory (CARO) (see Figure 2), of Eratosthenes Centre of Excellence and comprises the ACTRIS (Aerosols, Clouds and Trace gases Research InfraStructure) national facility of the Republic of Cyprus for the study of clouds and aerosols with remote sensing [18]. The station has been providing near-real time, 24/7 data of atmospheric aerosols and clouds vertical distribution since 2020. Polly^{XT} Lidar delivers vertical profiles of the particle backscatter coefficient at wavelengths 355, 532, 1064 nm. It also provides vertical measurements of the particle extinction coefficient, the volume and particle linear depolarization ratios and lidar ratios at 355 and 532 nm [4, 17].

Figure 2. CARO of Eratosthenes Centre of Excellence ground-based remote sensing station in Limassol, Cyprus.

Seven dust events were selected for this study. Desert dust cases were identified based on the exhibiting high attenuated backscatter coefficient and particle depolarization ratio, observed in the quick-look plots and the picks of the signal on the

vertical profiles available daily for each station on the PollyNet (Polly Lidar Network) platform of Polly Lidars (https://polly.tropos.de/, last accessed on 13 May 2025). High values of particle depolarization ratio indicate non-spherical aerosol particles which are characteristics of mineral dust. The cases filtered using the following criteria, cloud-free conditions to minimize signal contamination, a nighttime measurement to reduce the signal-to-noise ratio and to enable Raman measurements applied in the HETEAC-Flex model. Cases were limited which all necessary optical properties (extinction and backscatter coefficients at 355, 532, and 1064 nm, particle depolarization ratio and lidar ratio at 355, 532 nm) were available for the application of the six forward configuration modes, as detailed in Table 1. Layers were identified based on the features of the vertical profiles of backscatter coefficient, depolarization ratio and the altitude where the lidar ratio remained stable.

2.2 Limitations and Challenges

The data used in this analysis were the produced by the PollyNet automated processing chain. As the study's workflow depended on the availability of these automated products, this introduced additional limitations regarding the data completeness, unable to proceed with executing all the model six configuration modes. Due to the model execution the retrieval algorithm occasionally failed to converge within 30 iterations (the suggested), preventing the estimation of the optimal solution in some cases.

2.3 Case Study Analysis

The desert dust cases which satisfied the above criteria were analyzed further. The first characterization of the aerosol layers according to literature utilizing the mean values of the optical properties of the selected layers. HYSPLIT back-trajectories are used to identify the air mass origins and to confirm desert dust sources. Backscatter profiles from POLIPHON (polarization lidar–photometer networking) technique which separates backscatter contributions to mineral dust and non-dust [15] were used to confirm the aerosol layer and to classify if the mixture is dust or non-dust dominant. Satellite imagery from MODIS sensors on Aqua or Terra satellites were also employed to verify visually the presence of dust plume over the study area and in some cases the origin of the layer.

2.4 Application of HETEAC FLEX Model

HETEAC FLEX model was applied for the selected dust cases, to simulate aerosol mixture compositions. Relative volume contributions of predefined aerosol mixtures retrieved from the mode for each of the six forward configuration modes. For the validation of the forward configurations the consistency between the empirical data and the model outputs implemented and assess the modelled aerosol mixture representativeness. The results of the model evaluated for their statistical significance and compared with the independent analyses of each case (attenuated backscatter and depolarisation profiles, HYSPLIT, satellite images, POLIPHON backscatter profile, mean optical properties from POLLY^{XT} Lidar of the layer). This multi-tool validation approach enables the interpretation of desert dust events and enhances the reliability of the model regarding the characterization of aerosols.

3. RESULTS & DISCUSSION

HETEAC-Flex model applied to seven dust cases recorded in Limassol between the period 2021-2024, with the objective of identifying the optimal forward model configuration (set of optical properties) for accurately characterizing dust aerosol layers. A demonstration of detailed analysis of two representative case studies from dust cases originating from the Sahara and the Middle East is presented in this paper. For the two cases HETEAC-Flex model had apply and the comparison with the output of the analysis is presented below.

3.1 Case 1: Saharan Dust

3.1.1 Study of the case

On 8 September 2023, Polly^{XT} Lidar in Limassol captured a temporally stable, thick aerosol layer at heights between 1-3.5 km (see Figure 2 and Figure 3). Figure 3 shows the time-height cross section of the total attenuated backscatter coefficient at 1064nm (a) and volume depolarization ratio at 532 nm (b) measured from CARO Polly^{XT} Lidar on 08 September 2023 between 00:00-24:00 UTC. The evidence of the layer is indicated by the increased attenuated backscatter on vertical profile (see Figure 3). The time of the study of the selected layer is 20:00-21:00 at altitude 1-3 km.

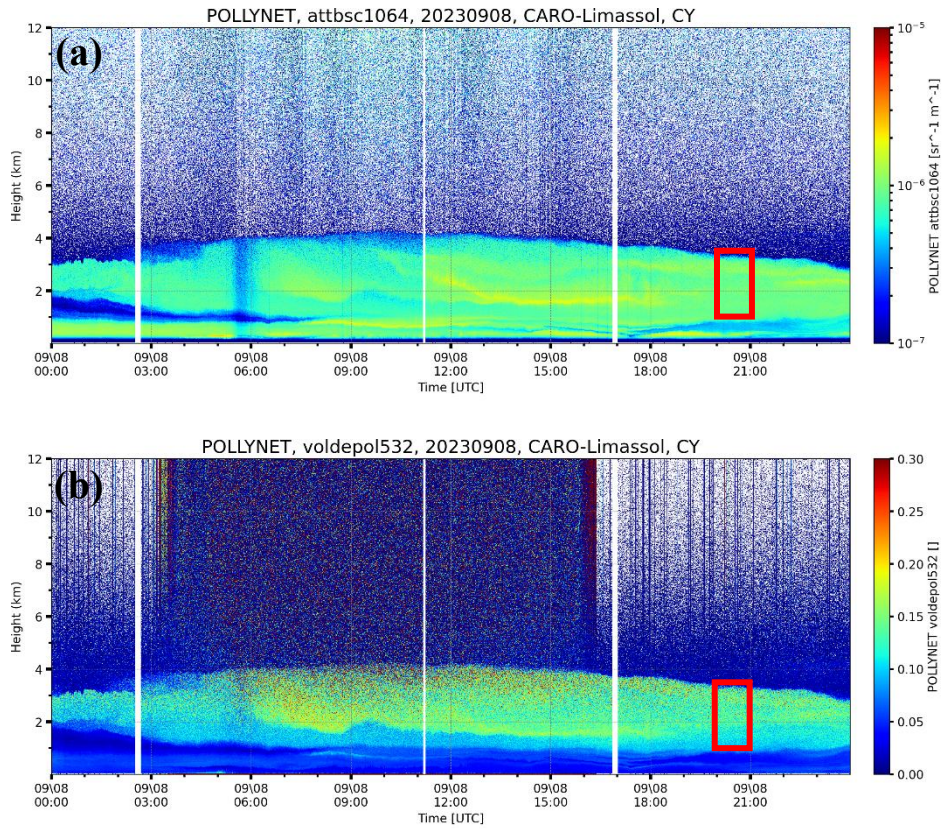

Figure 3. Time-height cross section of the (a) Total Attenuated Backscatter Coefficient at 1064nm and (b) Volume Depolarization Ratio at 532 nm measured from CARO Polly^{XT} Lidar on 08 September 2023, over Limassol, Cyprus. Red boarders indicate the region of the studied aerosol layer.

In Figure 4 the vertically resolved lidar-derived optical parameters retrieved from nighttime observations, between 20:00 - 21:00 UTC, and a vertical smoothing of 460 m are presented. For the studied layer (1-3 km) the particle linear depolarization ratio above 2 km at 532 nm exceeded 25%, indicating a strong presence of coarse mode particles. The maximum extinction coefficient observed was near 100 Mm^{-1}. The backscatter related Angstrom exponent (355/532 nm) was less than 1. The lidar ratio at 355 and 532 nm were stable for the core of the study aerosol layer at ≈ 40 sr with mean values 57.87 ± 5.04 sr and 43.73 ± 7.33 sr, respectively.

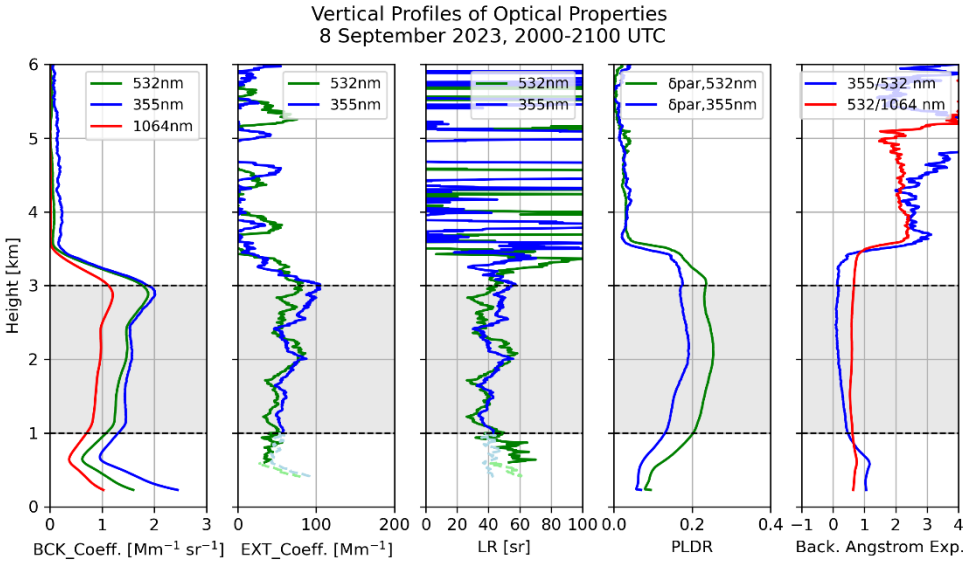

Figure 4. Vertical profiles of the backscatter coefficient, extinction coefficient, lidar ratio, particle depolarization ratio and backscatter related Angstrom exponent, measured in Limassol, Cyprus on 8 September 2023 from 20:00-21:00 UTC. Dashed lines indicate the near range lidar signal at 355 nm (light blue) and 532 nm (light green).

According to HYSPLIT model, in Figure 5 the 72-h backward trajectory arriving over Limassol, Cyprus (34.67 Nº, 33.02 Eº) at altitude 3 km at 20:00 UTC indicates that the airmass originated from Sahara Desert in North Africa (Egypt and Libya). Due to the path that air mass followed and because of the aerodynamic lifting, desert dust particles could be transported to Cyprus. Satellite imagery from the MODIS sensor on-board the AQUA satellite on that day 8 September 2023 clearly reveals intense atmospheric dust over the Limassol region.

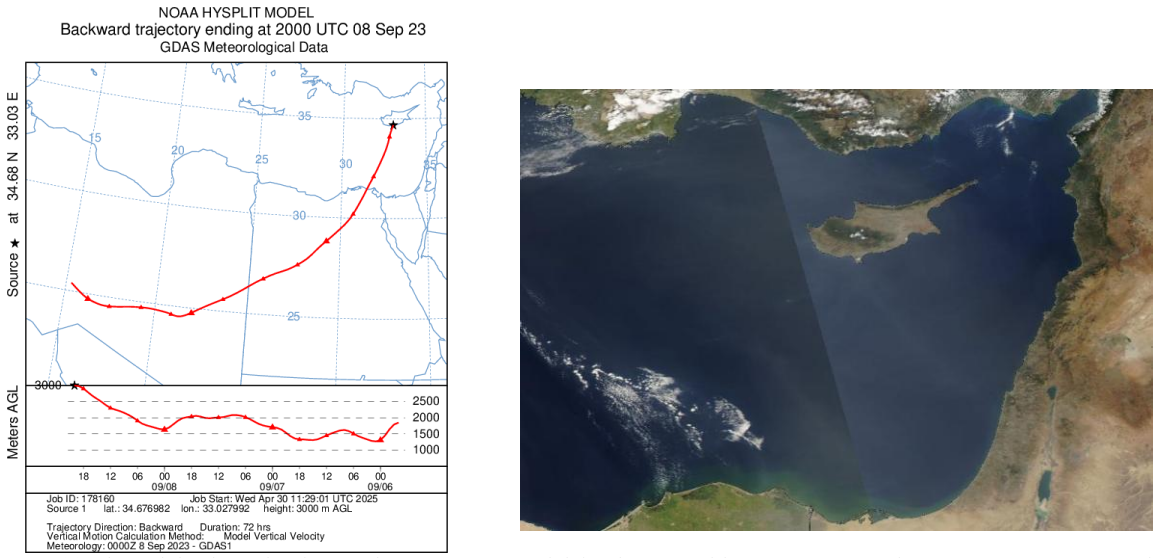

Figure 5. (a) The 72h backward trajectory by HYSPLIT model for the aerosol layer on 8 September 2023 at 20:00 UTC. The air mass is travelling from Sahara Desert to Cyprus. (b) Aqua/MODIS satellite image of Cyprus region, on 8 September 2023, (https://worldview.earthdata.nasa.gov/, last visit 09/05/2025).

In Figure 6, the Raman backscatter coefficient vertical profiles for 355, 532, 1064 nm and the one-step POLIPHON method Raman backscatter coefficient vertical profiles for dust and non-dust aerosols at 355, 532 nm are presented. From the scheme, the dust aerosol backscatter coefficient at 355, 532 nm exceeded the non-dust indicating the dominance of dust in the aerosol mixture.

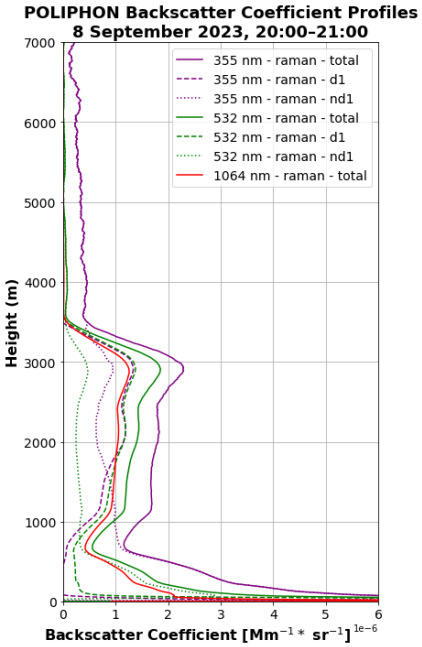

Figure 6. One-step POLIPHON vertical profiles of Raman backscatter coefficient for total (355 nm (purple), 532 nm (green) and 1064 nm (red)), dust (dashed line), and non-dust (dot line) aerosol components measured in Limassol, Cyprus, between 20:00 and 21:00 UTC on 8 September 2023.

Layer-averaged values of the optical properties of the atmospheric layer (1-3 km) needed for the application of the six forward model configurations of the HETEAC-flex model, on 8 September 2023 from Lidar, are presented in Table 2. The mean value of the particle linear depolarization ratios at 355 nm **(0.204 ± 0.017)** and 532 nm **(0.239 ± 0.012)** indicate the dominance of non-spherical aerosols in the layer.

Table 2. Saharan dust layer on 8 September 2023, mean optical properties from Lidar.

Properties from LIDAR	**Mean values layer**
δ_{355}	0.204 ± 0.017
S_{355}	57.9 ± 5.0
$A_{355/532}$	0.342 ± 0.388
δ_{532}	0.239 ± 0.012
S_{532}	43.7 ± 7.3
$C_{\beta 532/1064}$	1.36 ± 0.07

Based on a comprehensive analysis of observations and modelling tools the observed aerosol layer during the study period is predominantly composed of desert dust particles. The observations from Polly^{XT} lidar and the MODIS/Aqua satellite imagery identified an aerosol layer at altitude 1-3.5 km (layer height with Lidar). HYSPLIT model back-trajectories showed the origin of the air mass being Sahara Desert - North Africa. Mean optical properties of the layer derived from Polly^{XT} indicate high values of linear particle depolarization ratio and lidar ratio characteristics of desert dust (see Table 2) [19].

3.1.2 Aerosol typing with HETEAC-Flex

As input to HETEAC-Flex model for retrieval mode 1, mean values of the particle linear depolarization ratio (20.4 ± 2 %) and lidar ratio (58 ± 5) at 355 nm of the layer were used as summarized in Table 2. For this mode the initial guess - state vector based on decision tree of input data and the optimal solution is CNS – desert dust dominated mixture. The dominance of CNS aerosol is confirmed by that retrieval configuration mode 1 which is also statistically significant within 95% confidence interval (Figure 7).

CNS components accounted for 97.69 ± 22.36% of the total atmospheric aerosol mixture in terms of relative volume contribution (see Table 3). The residual aerosol components contributed minimally as 0.17 ± 7.86% for FSA, 0.78 ± 17.78% for CS and 1.36 ± 11.23% for FSNA. The dominant aerosols of the mixture are the coarse-mode particles.

The optimal solutions for the rest of the retrieval modes (see Table 1 and Table 3) were not statistically significant (Figure 7b, c, d, e, f), thus the retrievals of the model consistently reflected the dominance of the CNS aerosol component for (89.57 ± 22.26%, 97.74 ± 22.36%, 62.33 ± 20.91%, 89.44 ± 22.3%, 87.18 ± 22.22%) for retrieval modes 2, 3, 4, 5, 6 respectively.

Table 3. Relative volume contribution of four aerosol components from HETEAC-Flex model on 8 September 2023.

Retrieval mode	FSA	CS	FSNA	CNS
Mode 1	0.17 ± 7.86	0.78 ± 17.78	1.36 ± 11.23	97.69 ± 22.36
Mode 2	0 ± 10.68	10.17 ± 12.32	0.08 ± 16.18	89.57 ± 22.26
Mode 3	0 ± 5.61	0 ± 11.98	2 ± 7.58	97.74 ± 22.36
Mode 4	0 ± 9.41	0 ± 10.65	27.13 ± 12.96	62.33 ± 20.91
Mode 5	1.64 ± 3.37	7.85 ± 5.58	0 ± 4.87	89.44 ± 22.3
Mode 6	3.05 ± 2.96	9.51 ± 5.28	0 ± 4.41	87.18 ± 22.22

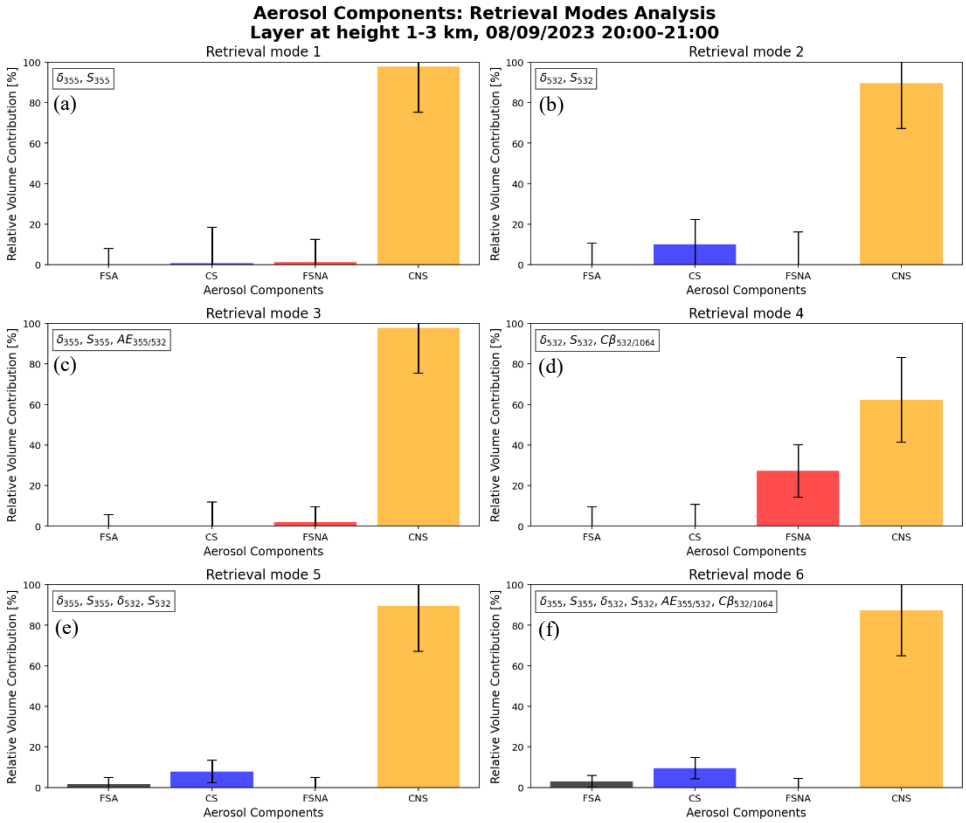

Figure 7. Mixing state, relative volume contribution [%] of the four aerosol components retrieved by HETEAC-Flex model for all the retrieval modes, for the 1-3 km atmospheric layer over Limassol, Cyprus on 08 September 2023 between 20:00 and 21:00 UTC.

Retrieval mode 1, which integrates the particle linear depolarization ratio and lidar ratio at 355 nm, is considered the optimal forward configuration mode for the identification of relative volume contribution of aerosol components for this case study.

3.2 Case 2: Middle East

3.2.1 Study of the case

On 29 April 2024, a thick, temporally stable aerosol layer at heights between 0.5-4 km (see Figure 8 and Figure 9) captured by Polly^{XT} Lidar in Limassol. Figure 8 shows the time-height cross section of the total attenuated backscatter coefficient at 1064nm (a) and volume depolarization ratio at 532 nm (b) measured from CARO Polly^{XT} Lidar on 29 April 2024 between 00:00-24:00 UTC. The evidence of the layer is indicated by the increased attenuated backscatter on vertical profile (see Figure 9). The analysis of the selected layer was conducted between 00:00-00:59 at height range 1-4 km.

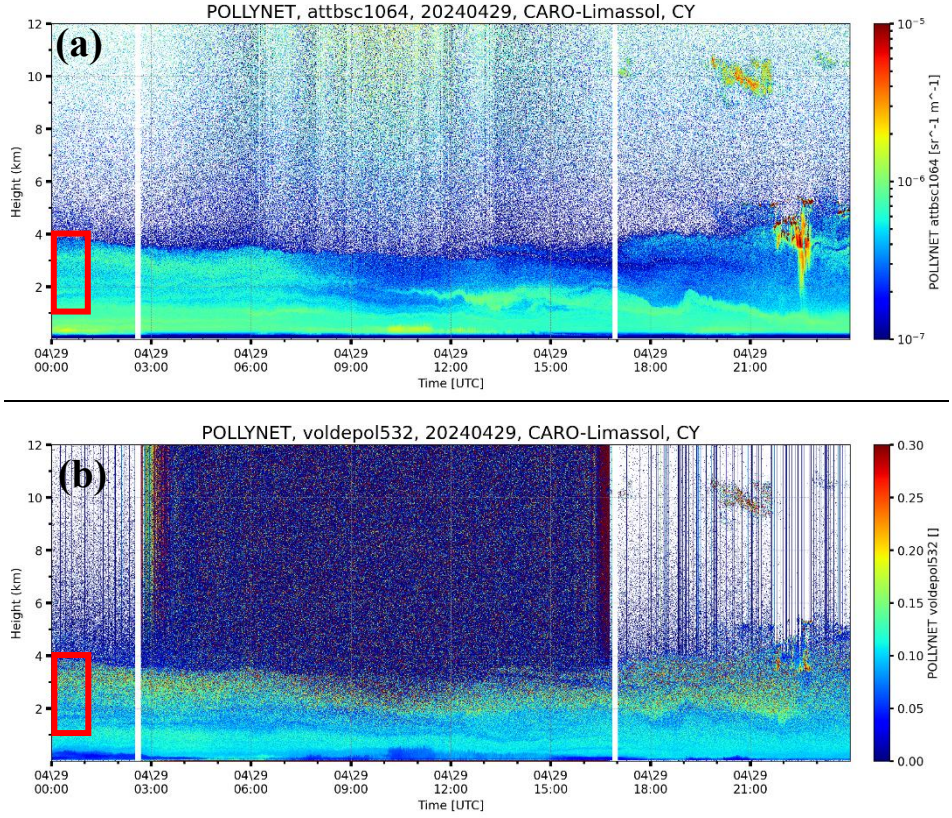

Figure 8. Polly^{XT} lidar (a) Attenuated backscatter at 1064 nm (b) Volume linear depolarization ratio at 532 nm over Limassol, Cyprus, on 29 April 2024. Red boarders indicate the region of the studied aerosol layer.

In Figure 9, (between 00:00-00:59) are presented the vertically resolved lidar-derived optical parameters retrieved from nighttime observations, with a vertical smoothing of 460 m are presented. For the studied layer (1-4 km) the particle linear depolarization ratio above 2.5 km at 355 and 532 nm exceeded 25%, indicating a strong presence of coarse mode particles indicative value for dust. The maximum extinction coefficient observed was near 80 Mm^{-1}. The lidar ratio at 355 and 532 nm were stable for the core of the study aerosol layer (1-3.5 km) at ≈ 50 sr with mean values 56.2 ± 13 sr and 45.5 ± 17 sr, respectively.

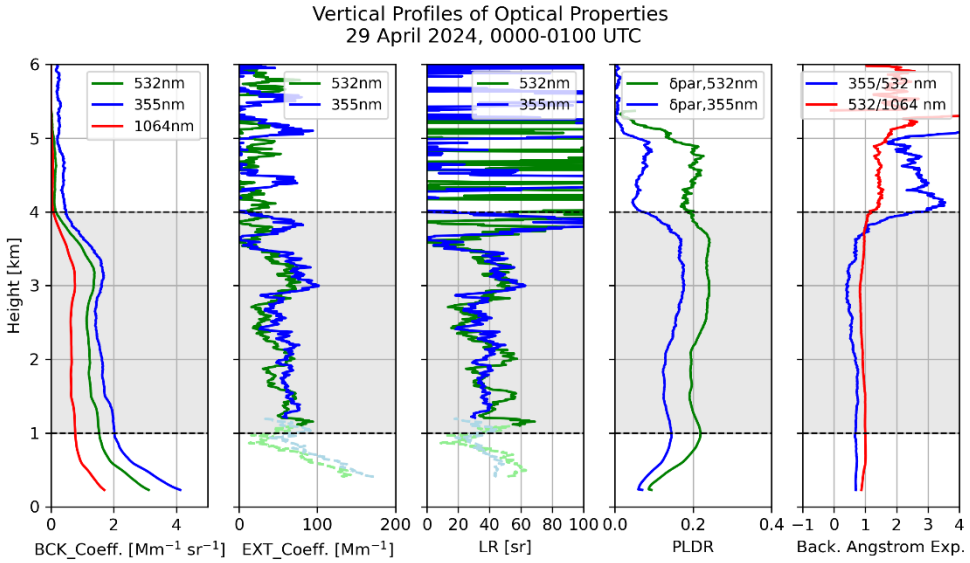

Figure 9. Vertical profiles of the backscatter coefficient, extinction coefficient, lidar ratio, particle depolarization ratio and backscatter related Angstrom exponent, measured in Limassol, Cyprus on 29 April 2024 from 00:00-01:00 UTC. Dashed lines indicate the near range lidar signal at 355 nm (light blue) and 532 nm (light green).

A 72-h backward trajectory from the HYSPLIT model, arriving over Limassol, Cyprus (34.67 N°, 33.02 E°) at altitude 2.5 km at 01:00 UTC indicates that the airmass originated from Middle East, Arabian Peninsula (see Figure 10a). Desert dust particles due to the wind path that air mass could be transported to Cyprus. Dust and clouds over the Limassol region were observed from the satellite imagery from the MODIS sensor on-board the AQUA satellite (see Figure 10b).

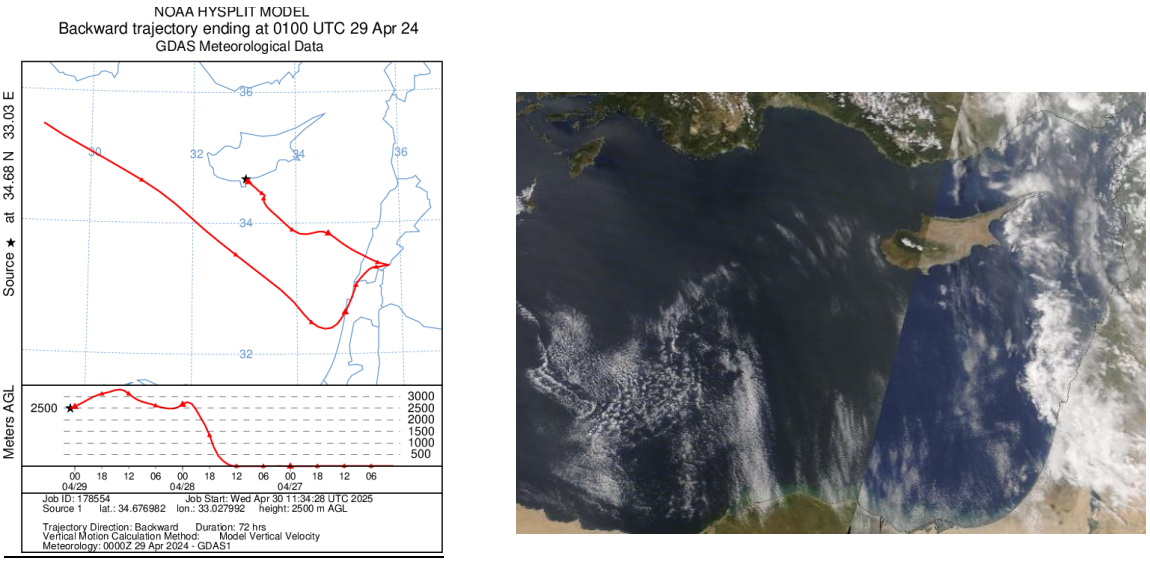

Figure 10. (a) The 72h backward trajectory by HYSPLIT model for the aerosol layer on 29 April 2024 at 01:00 UTC. The air mass is travelling from Middle East Desert to Cyprus. (b) Aqua/MODIS satellite image of Cyprus region on 29 April 2024, (https://worldview.earthdata.nasa.gov/, last visit 05/09/2025).

In Figure 11, the Raman total backscatter coefficient vertical profiles at 532 nm and the one-step POLIPHON method Raman backscatter coefficient vertical profiles for dust and non-dust aerosols at 532 nm are presented. Dust aerosol Backscatter coefficient at 532 nm surpassed the non-dust indicating the predominance of dust in the aerosol composition.

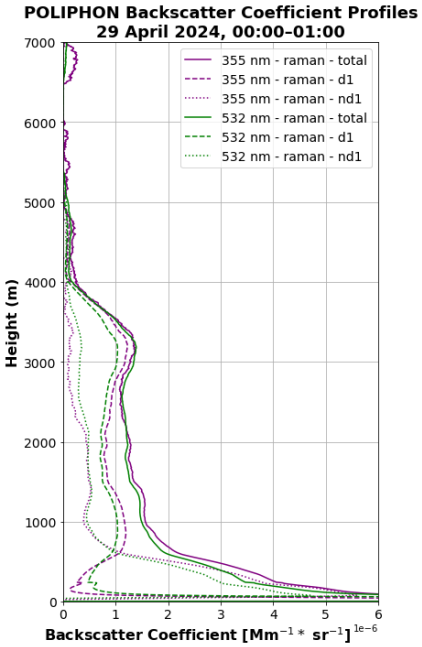

Figure 11. One-step POLIPHON vertical profiles of Raman backscatter coefficient for total (355 nm (purple), 532 nm (green), dust (dashed line), and non-dust (dot line) aerosol components measured in Limassol, Cyprus, between 00:00 and 01:00 UTC on 29 April 2024.

In Table 4 the layer-averaged values of the optical properties of the atmospheric layer (1-4 km) from Lidar needed for the application of the six forward model configurations of the HETEAC-flex model are presented.
The mean value of the particle linear depolarization ratios at 355 nm (0.202 ± 0.045) and 532 nm (0.219 ± 0.019) indicate the dominance of non-spherical aerosols in the layer.

Table 4. Middle East dust layer on 29 April 2024, mean optical properties from Lidar.

Properties from LIDAR	Mean values layer
δ_{355}	0.202 ± 0.045
S_{355}	56.2 ± 13.0
$A_{355/532}$	0.355 ± 1.21
δ_{532}	0.219 ± 0.019
S_{532}	45.5 ± 17.0
Cβ532/1064	1.82 ± 0.12

From the synergy of observations and modelling tools the observed aerosol layer during the study period the comprehensive analysis showed that the dominant composition is desert dust. The observations from Polly^{XT} lidar and the MODIS/Aqua satellite imagery identified an aerosol layer at altitude 0.5-4 km (the layer height with lidar). HYSPLIT model back-trajectories showed the origin of the air mass being Middle East. High values of linear particle depolarization ratio and lidar ratio of the optical properties of the layer from Polly^{XT} indicate characteristics of desert dust (see Table 4) [19].

For the forward configuration mode 1of the HETEAC-Flex model, the input parameters included the layer averaged particle linear depolarization ratio (20.2 ± 4.5 %) and lidar ratio (56 ± 13) at 355 nm were used (see Table 4). In retrieval

mode 3, the same input parameters were employed with addition the Extinction-related Angstrom exponent at 355/532 nm 0.355 ± 1.2.

3.2.2 Aerosol typing with HETEAC-Flex model

The initial guess - state vector based on decision tree of input data of all the configuration modes and the optimal solution were CNS – desert dust dominated mixture. The solutions of the retrieval configuration modes 1 and 3 were also statistically significant within 95% confidence interval (Figure 12a, c) confirming that the cases were CNS aerosol dominant. CNS components for retrieval mode 1, accounted for 97.07 ± 22.36% and for retrieval mode 3 97.31 ± 22.36% of the total atmospheric aerosol mixture in terms of relative volume contribution (see Table 5). The residual aerosol components contributed minimally as summarized in Table 4. The dominant aerosols of the mixture are the coarse-mode particles.

The optimal solutions for the rest of the retrieval modes (see Table 1and Table 5) were not statistically significant (Figure 12b, d, e, f). The model outcomes indicated that CNS aerosol was the dominant component in retrieval modes 1, 2, 3, 5. In contrast, retrieval modes 4, 6 characterized by mixture of CNS and FSNA aerosols with Fine Spherical non-absorbing aerosols being the prevailing type which contradicts the analysis presented above.

Table 5. Relative volume contribution of four aerosol components from HETEAC-Flex model on 29 April 2024.

Retrieval mode	FSA	CS	FSNA	CNS
Mode 1	0 ± 8.54	1.13 ± 17.93	1.56 ± 11.49	97.07 ± 22.36
Mode 2	0 ± 12.55	7.37 ± 14.33	4.26 ± 16.31	87.73 ± 22.27
Mode 3	0 ± 8.32	0.17 ± 16.89	2.13 ± 10.82	97.31 ± 22.36
Mode 4	0 ± 17.39	0 ± 18.06	50 ± 18.41	37.81 ± 14.77
Mode 5	1.74 ± 7.35	10.32 ± 10.55	0 ± 10.51	87.31 ± 22.28
Mode 6	0 ± 14.49	0 ± 17.91	54.11 ± 18.59	39.31 ± 14.42

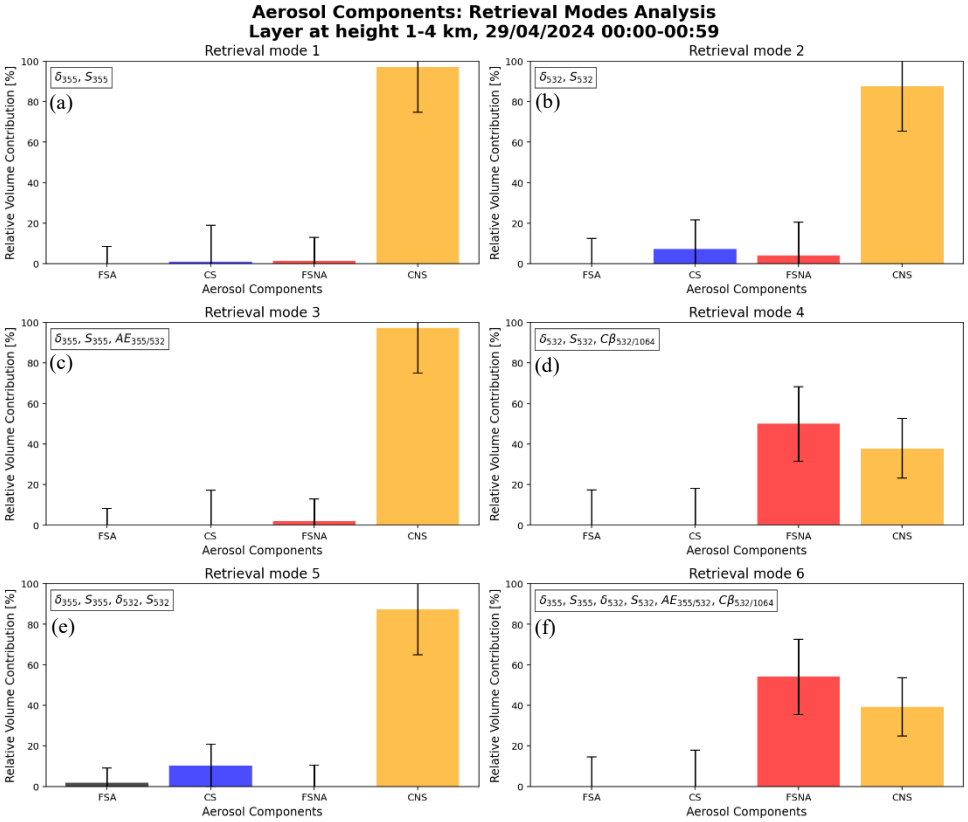

Figure 12. Mixing state, relative volume contribution [%] of the four aerosol components retrieved by HETEAC-Flex model for all the retrieval modes, for the layer 1- 4 km atmospheric layer over Limassol, Cyprus on 29 April 2024 between 00:00 and 00:59.

Forward model configurations 1 and 3 which use particle linear depolarization ratio, lidar ratio at 355 nm and Extinction-related Angstrom exponent at 355/532 nm considered the optimal forward configuration modes for the identification of relative volume contribution of aerosol components for this case study.

4. CONCLUSIONS

This study demonstrated the application of the HETEAC-Flex model to several dust cases recorded in Limassol from Polly^{XT} lidar observations between the period 2021-2024, aiming to determine which configuration mode of the model is the optimal for characterizing dust aerosol layers. Two desert dust events originating from Sahara Desert and Arabian Peninsula are presented in this paper. The results of the model and the analysis confirmed that both cases were dominated by Coarse Non-Spherical aerosol particles, typical characteristics of mineral desert dust.

Across the configurations tested, retrieval modes 1,2 and 3 yielded the most consistent and statistically significant results. Retrieval mode 1, which utilized particle linear depolarization ratio and lidar ratio at 355 nm from lidar observations, in most cases produced statistically significant results. Both cases presented in this paper accurately identify Coarse Non-Spherical as primary aerosol component. Middle East case showed that also forward configuration mode 3 which incorporates also the extinction-related Ångström exponent at 355/532 nm as an input to the model, had a statistically significant solution and provided reliable results. Also, the solution in some cases of the retrieval mode 2 of the model which incorporates the particle linear depolarization ratio and lidar ratio at 532 nm were statistically significant and the results were comparable to those of the modeling tools and observational analysis.

In contrast, the solutions of retrieval modes 4 and 6 were frequently statistically insignificant and occasionally led to aerosol misclassification highlighting the limitations of these configurations for the desert dust layers. Based on the findings, retrieval mode 1 (δ_{355}, S_{355}) is recommended as a reliable option for EarthCARE aerosol classification products validation in dust-dominated conditions.

ACKNOWLEDGEMENTS

The study is supported by the 'EXCELSIOR': ERATOSTHENES: EXcellence Research Centre for Earth Surveillance and Space-Based Monitoring of the Environment H2020 Widespread Teaming project (www.excelsior2020.eu). The 'EXCELSIOR' project has received funding from the European Union's Horizon 2020 research and innovation programme under Grant Agreement No 857510, from the Government of the Republic of Cyprus through the Directorate General for the European Programmes, Coordination and Development and the Cyprus University of Technology. The authors acknowledge the ATARRI project funded by the European Union's Horizon Europe Twinning Call (HORIZON-WIDERA-2023-ACCESS-02) under the grant agreement No 101160258.

REFERENCES

[1] Floutsi, A. A., Baars, H., and Wandinger, U., "HETEAC-Flex: an optimal estimation method for aerosol typing based on lidar-derived intensive optical properties," *Atmos. Meas. Tech.*, 17(1), 693–714 (2024). https://doi.org/10.5194/amt-17-693-2024

[2] Achilleos, S., Mouzourides, P., Kalivitis, N., Katra, I., Kloog, I., Kouis, P., Middleton, N., Mihalopoulos, N., Neophytou, M., Panayiotou, A., Papatheodorou, S., Savvides, C., Tymvios, F., Vasiliadou, E., Yiallouros, P., and Koutrakis, P., "Spatio-temporal variability of desert dust storms in Eastern Mediterranean (Crete, Cyprus, Israel) between 2006 and 2017 using a uniform methodology," *Sci. Total Environ.*, 714, 136693 (2020). https://doi.org/10.1016/j.scitotenv.2020.136693

[3] Pikridas, M., Vrekoussis, M., Sciare, J., Kleanthous, S., Vasiliadou, E., Kizas, C., Savvides, C., and Mihalopoulos, N., "Spatial and temporal (short and long-term) variability of submicron, fine and sub-10 μm particulate matter (PM1, PM2.5, PM10) in Cyprus," *Atmos. Environ.*, **191**, 79–93 (2018). https://doi.org/10.1016/j.atmosenv.2018.07.048

[4] Mamouri, R.-E., Ansmann, A., Ohneiser, K., Knopf, D. A., Nisantzi, A., Bühl, J., Engelmann, R., Skupin, A., Seifert, P., Baars, H., Ene, D., Wandinger, U., and Hadjimitsis, D., "Wildfire smoke triggers cirrus formation: lidar observations over the eastern Mediterranean," *Atmos. Chem. Phys.*, 23(21), 14097–14114 (2023). https://doi.org/10.5194/acp-23-14097-2023

[5] Mamouri, R. E., Ansmann, A., Nisantzi, A., Kokkalis, P., Schwarz, A., and Hadjimitsis, D., "Low Arabian dust extinction-to-backscatter ratio," *Geophys. Res. Lett.*, 40(19), 4762–4766 (2013). https://doi.org/10.1002/grl.50898

[6] Mamouri, R.-E., Ansmann, A., Nisantzi, A., Solomos, S., Kallos, G., and Hadjimitsis, D. G., "Extreme dust storm over the eastern Mediterranean in September 2015: satellite, lidar, and surface observations in the Cyprus region," *Atmos. Chem. Phys.*, 16(21), 13711–13724 (2016). https://doi.org/10.5194/acp-16-13711-2016

[7] Nisantzi, A., Mamouri, R. E., Ansmann, A., and Hadjimitsis, D., "Injection of mineral dust into the free troposphere during fire events observed with polarization lidar at Limassol, Cyprus," *Atmos. Chem. Phys.*, 14(22), 12155–12165 (2014). https://doi.org/10.5194/acp-14-12155-2014

[8] Nisantzi, A., Mamouri, R. E., Ansmann, A., Schuster, G. L., and Hadjimitsis, D. G., "Middle East versus Saharan dust extinction-to-backscatter ratios," *Atmos. Chem. Phys.*, 15(13), 7071–7084 (2015). https://doi.org/10.5194/acp-15-7071-2015

[9] Ansmann, A., Mamouri, R.-E., Hofer, J., Baars, H., Althausen, D., and Abdullaev, S. F., "Dust mass, cloud condensation nuclei, and ice-nucleating particle profiling with polarization lidar: updated POLIPHON conversion factors from global AERONET analysis," *Atmos. Meas. Tech.*, 12(9), 4849–4865 (2019). https://doi.org/10.5194/amt-12-4849-2019

[10] Wandinger, U., Floutsi, A. A., Baars, H., Haarig, M., Ansmann, A., Hünerbein, A., Docter, N., Donovan, D., van Zadelhoff, G.-J., Mason, S., and Cole, J., "HETEAC – the Hybrid End-To-End Aerosol Classification model for EarthCARE," *Atmos. Meas. Tech.*, **16**(5), 2485–2510 (2023). https://doi.org/10.5194/amt-16-2485-2023

[11] Wandinger, U., et al., "HETEAC: The aerosol classification model for EarthCARE," *EPJ Web Conf.*, 119, 01004 (2016). https://doi.org/10.1051/epjconf/201611901004

[12] Rodgers, C. D., *Inverse methods for atmospheric sounding: theory and practice*, Vol. 2, World Scientific (2000). https://doi.org/10.1142/3171

[13] Román, R., et al., "Retrieval of aerosol properties using relative radiance measurements from an all-sky camera," *Atmos. Meas. Tech.*, 15(2), 407–433 (2022). https://doi.org/10.5194/amt-15-407-2022

[14] Tesche, M., Ansmann, A., Müller, D., Althausen, D., Engelmann, R., Freudenthaler, V., and Groß, S., "Vertically resolved separation of dust and smoke over Cape Verde using multiwavelength Raman and polarization lidars during Saharan Mineral Dust Experiment 2008," J. Geophys. Res.-Atmos., 114(D13), D13202 (2009). https://doi.org/10.1029/2009JD011862

[15] Mamouri, R. E., and Ansmann, A., "Fine and coarse dust separation with polarization lidar," *Atmos. Meas. Tech.*, 7(12), 3717–3735 (2014). https://doi.org/10.5194/amt-7-3717-2014

[16] Heese, B., et al., "The vertical aerosol type distribution above Israel – 2 years of lidar observations at the coastal city of Haifa," *Atmos. Chem. Phys.*, 22(3), 1633–1648 (2022). https://doi.org/10.5194/acp-22-1633-2022

[17] Engelmann, R., et al., "The automated multiwavelength Raman polarization and water-vapor lidar PollyXT: the neXT generation," *Atmos. Meas. Tech.*, 9(4), 1767–1784 (2016). https://doi.org/10.5194/amt-9-1767-2016

[18] ACTRIS, "Aerosols, Clouds and Trace gases Research InfraStructure home page," https://www.actris.eu/, last access: 16 May 2025.

[19] Floutsi, A. A., et al., "DeLiAn – a growing collection of depolarization ratio, lidar ratio and Ångström exponent for different aerosol types and mixtures from ground-based lidar observations," *Atmos. Meas. Tech.*, 16(6), 2353–2379 (2023). https://doi.org/10.5194/amt-16-2353-2023